VTT Technical Research Centre of Finland

RANS predictions for flow patterns around a compact azipod

Sanchez Caja, Antonio; Pylkkänen, Jaakko V.

Published in:
Proceedings in 2nd International conference on technical advances in Podded propulsion

Published: 01/01/2006

Document Version
Publisher's final version

RANS PREDICTIONS FOR FLOW PATTERNS AROUND A COMPACT AZIPOD

Antonio Sánchez-Caja, VTT, Finland
Jaakko V. Pylkkanen, VTT, Finland

VTT has numerically investigated the hydrodynamic performance of a Compact Azipod unit at full and model scale at the design operation point. VTT used RANSE (Reynolds-Averaged-Navier-Stokes Equation) solver FINFLO in the calculations. Scale effects are shown for the forces on different components of the unit. Pressure distributions and streamlines are presented to illustrate regions of 3D separation on the strut and pod.

1. Introduction

This paper presents the CFD analysis of the flow around a Compact Azipod unit for the design condition at both full scale and model scale. The RANS solver FINFLO was used in this work. FINFLO has been earlier applied to the analysis of the flow around a podded propulsor at full and model scale [1] and [2]. In these earlier occasions the pod was of tubby form. In the present case the geometric form of the housing is not quite conventional either. The Compact Azipod unit consists of a propeller, a pod, and a strut that is connected to the rear part of the pod at an angle about 45 degrees relative to the rotation axis of the propeller.

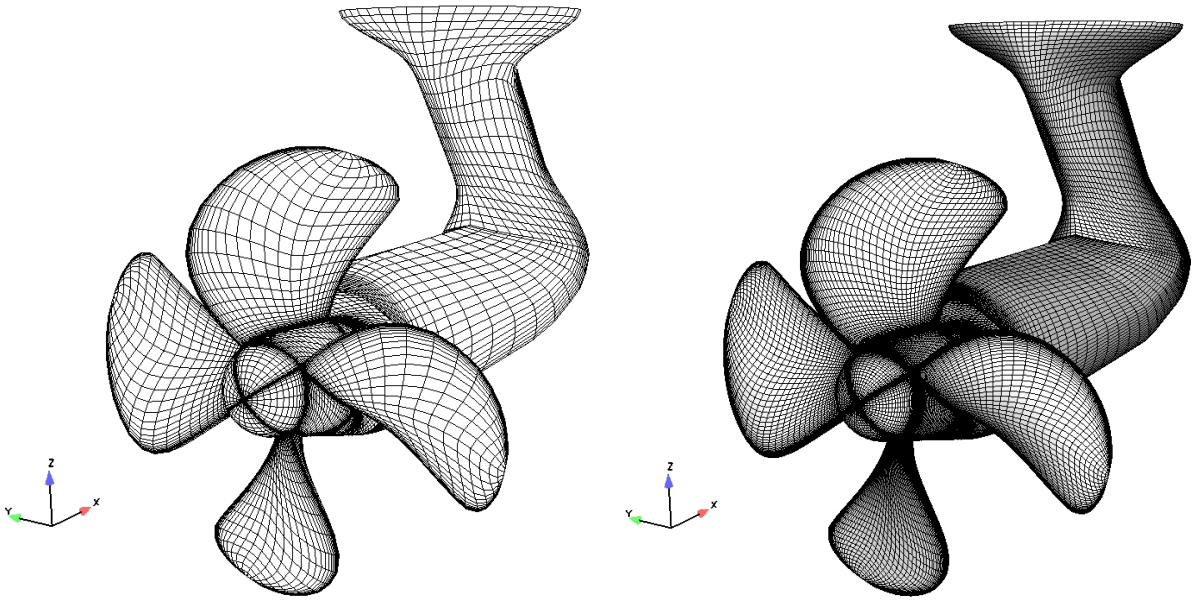

(a) Coarse grid *(b) fine grid*

Figure 1. Surface grids for compact Azipod. Front view.

Section 2 of this paper describes the geometry of the propulsor under investigation. Sections 3 and 4 describe briefly the calculations. The results are given in Sections 5 and 6. Sections 7 and 8 present a short discussion and conclusion, respectively.

2. Description of geometry

The propeller of the Compact Azipod unit under investigation is a 4-bladed one with moderate skew. The diameter is 2.5 m. The model scale was selected as 1:11.4 for the RANS calculation. However, no model Azipod has been manufactured and no model tests have been performed. The Compact Azipod unit under investigation can best be visualized by looking at Figures 1 and 2.

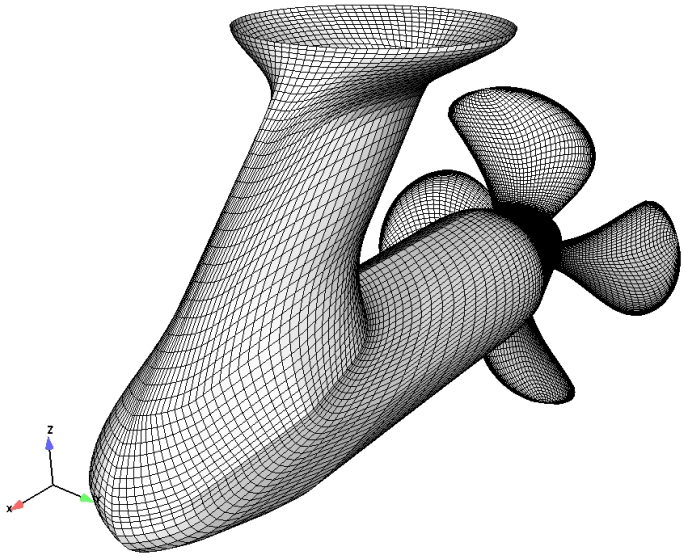

Figure 2. Surface grids for compact Azipod. Rear view.

3. Numerical method

Calculations with FINFLO can be made in three different forms; time-accurate, time-average, and quasi-steady. For the present study the quasi-steady approach was chosen to account for the lack of axial symmetry in the flow around the propeller blades due to the presence of the strut. This approach focuses on a single position of the propeller and does not take into account memory effects present in the time-accurate method. The selected propeller position was that of one blade at the 12.00 position.

The computations were performed on a cluster of PC. Chien's low Reynolds k-epsilon turbulence model was used. A detailed description of the computational method can be found in [3]. The ENSIGHT program was used for post-processing the output files.

4. Calculations

The computations were made using coarse grids of 0.6 million cells and fine grids of 4.9 million cells. H-topology was chosen around the propeller blades and O-topology around the pod and strut. Figure 1a and 1b shows respectively the front view of the coarse and fine grid on the Azipod surfaces. Figures 2 show the fine grid from a rear view. The housing geometry was given to VTT in IGES format. For the

calculations pod geometry was simplified in such a way that the cooling openings on the pod surface were not modeled. The computational mesh was generated with IGG software.

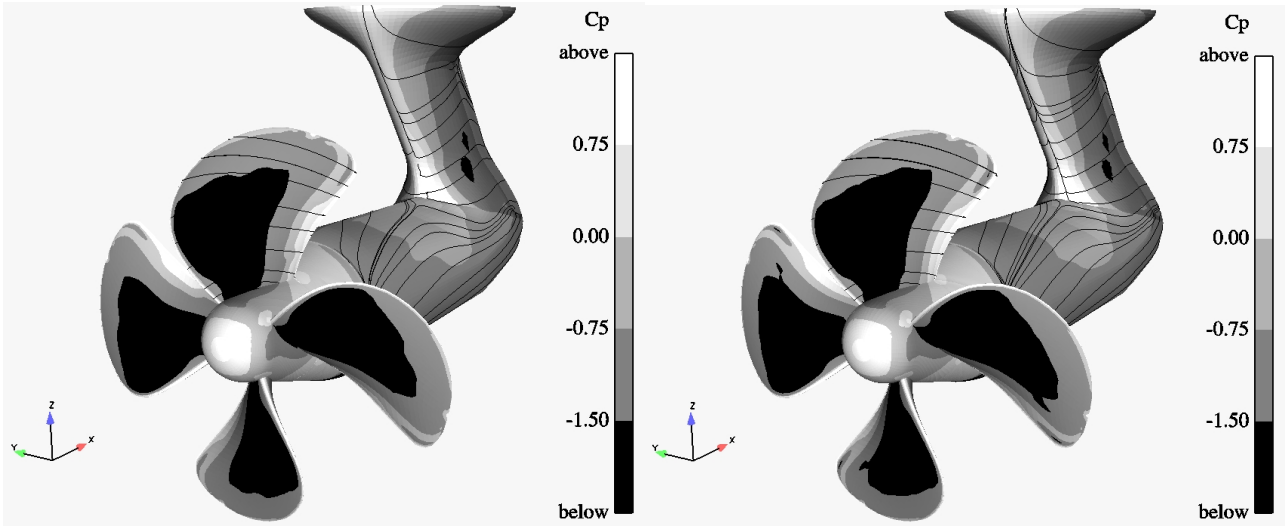

(a) model scale *(b) full scale*

Figure 3. Front view of the pressure distribution and streamlines for a Compact Azipod unit.

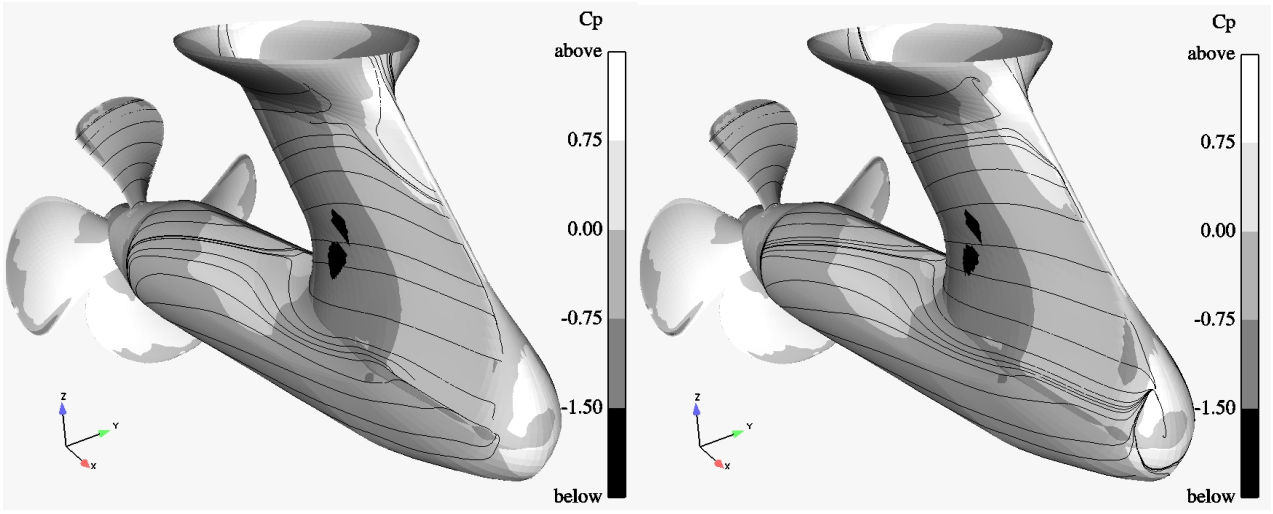

(a) model scale *(b) full scale*

Figure 4. Rear view of the pressure distribution and streamlines for a Compact Azipod unit. Port side.

The calculations were made using two multi-grid levels for the design operation point conditions. The propeller forces converged fast, in about 3000-5000 iterations. However, the drag forces on the pod converged more slowly due to the presence of flow detachment. The slowness of convergence was more apparent in the full scale calculation. It was related to the calculation of the separation areas: the

separation areas were moving to its final shape slowly due to the very small cells within the boundary layer.

5. Results: Pressure distributions and streamlines

A front view of the pressure distribution and streamlines is shown for model and full scale calculations in Figures 3a and 3b respectively; and a back view in Figures 4a and 4b for the port side, and in Figures 5a and 5b for the starboard side. All the results correspond to the fine grid. Qualitatively speaking, the pressure distributions are similar in the full and model scale calculations. Some differences can be observed in the high pressure areas on the rear part of the pod. For the streamlines the tendency is the same as that shown in ref. [1], i.e. the separation areas are smaller at full scale than at model scale, which results in a decrease of resistance for the full scale pod.

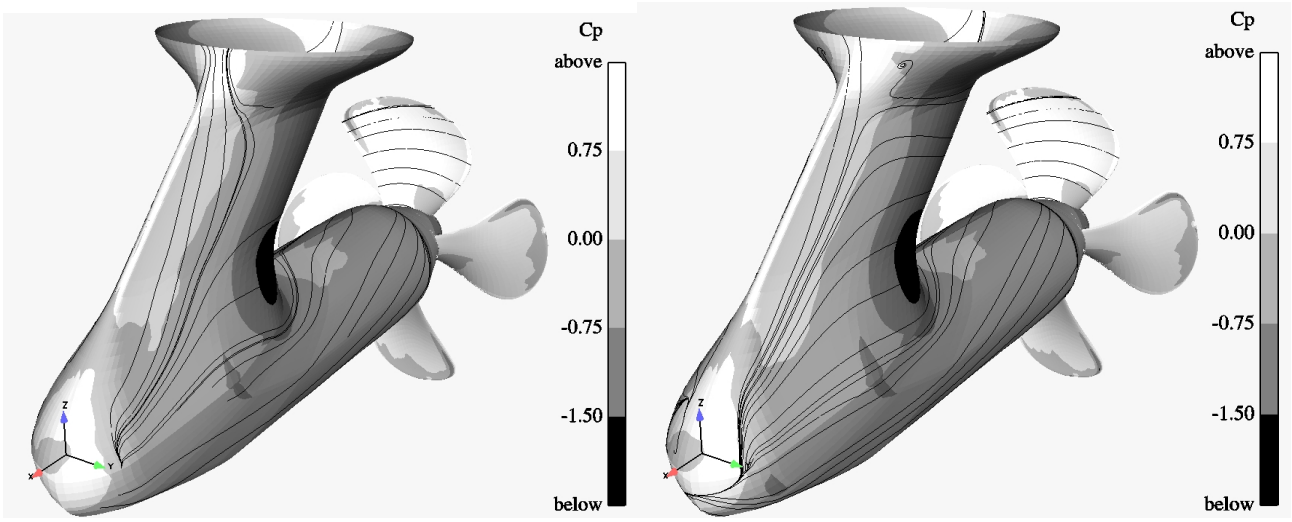

(a) model scale *(b) full scale*

Figure 5. Rear view of the pressure distribution and streamlines for a Compact Azipod unit. Starboard side.

6. Results: Forces and moments

Table I shows the change predicted by FINFLO in the performance coefficients from model to full scale as percentages of the model scale values. The unit thrust coefficient is expected to increase by 7.1 percent, the torque by 1.0 and the efficiency by 6.1.

Table II shows a comparison of the thrusting forces acting on each component of the propulsor unit relative to the model scale unit thrust. The separation line between pod and strut is not evident for the Compact Azipod unit. In the RANS simulation the definition of pod and strut was made by choosing as separation line the grid line shown in Figures 1a and 1b at the intersection of pod and strut at the front

symmetry plane, which is clearly defined. Consequently the strut component contains also what would be the upper part of the rear pod in other more conventional podded unit configurations.

Table I. Comparison of performance coefficients for the tractor thruster. Model versus full scale.

scale	**full**	**model**
Kt-unit	107.1	100
Kt-blades	104.9	100
Kq	101.0	100
η-unit	106.1	100
η-blades	103.9	100

The full scale force coefficient for the propeller blades is predicted 15.8 percent larger than the model scale unit thrust coefficient, which means 8.1 percent (=115.8/107.1) larger than the full scale unit thrust. The model scale force coefficient for the propeller blades is 10.4 percent larger than the model scale unit thrust. Comparing the 8.1 percent to the 10.4 percent the propeller blade is 2.3 percent more loaded at model scale than at full scale in relative terms of the unit thrust, which corresponds to a 5 percent (=115.8/110.4) larger loading in absolute terms. This information can be useful for example when setting the right propeller loading in cavitation tests.

Table II. Comparison of axial force coefficients over the components of the thruster. Model versus full scale.

scale	**full**	**model**
propeller blades	115.8	110.4
strut	-3.7	-4.5
pod	-5.0	-5.9
Total	107.1	100.0
blades + rotating hub	114.2	108.6
non-rotating parts	-7.1	-8.6
Total	107.1	100.0

Table II also shows for the propulsor unit the relative contribution of the rotating and non-rotating parts to the thrust (or drag) in the calculation. The drag coefficient of the non-rotating parts of the housing decreased from 8.6 to 7.1 percent of the model scale unit thrust, i.e. the full scale drag coefficient was 82 percent of that at model scale. In relative terms of the unit drag the drag coefficient of the non-rotating parts decreased from 8.6 to 6.6 (=100*7.1/107.1), i.e. the full scale drag coefficient was 77 percent of that at model scale.

It should be noted that the scale ratio between the model scale and full scale calculation (1:11.4) is not very large (for example, in [4] the scale was 1:23.33). For larger ratios the quotient between the full

scale and model scale drag coefficients is expected to further decrease as a consequence of both reduction of flow separation and frictional resistance.

From the figures in Table II it can be seen that the (rotating and non-rotating) pod drag coefficient was reduced by 15 percent and the strut drag coefficient by 18 percent. Comparing both numbers, the reduction of flow separation areas on the strut results in an increase of its lifting properties under an oblique flow. This effect produces a further drag reduction on the strut, not present on the pod. This was also the case for the strut of the housing of [1].

Table III. Frictional resistance as relative percentage of the total resistance of each component.

scale	**full**	**model**
propeller blades	-1.5	-1.7
strut	28.4	31.0
pod	33.7	42.6
rotating parts	-1.9	-2.2
stationary parts	34.3	40.0

Table III shows in percentages the relative contribution of frictional forces to total forces for each component of the propulsor. For instance, the full scale frictional resistance for the strut profile is 28 percent of the total one and consequently the pressure resistance is 72 percent. The relative small and negative percentages for the propeller blades (or rotating parts) are due to the fact that the propeller blades are providing not only drag as the other components do but also a large pressure-based thrust (negative drag). The contribution of the frictional forces to the total resistance is less at full scale.

Table IV. Frictional and pressure resistance as absolute percentage of the model unit thrust.

scale	**full**		**model**	
%	**Cf**	**Cp**	**Cf**	**Cp**
propeller blades	-1.8	117.6	-1.9	112.3
strut	-1.0	-2.7	-1.4	-3.1
pod	-1.7	-3.3	-2.5	-3.4
rotating parts	-2.1	116.3	-2.4	111.0
stationary parts	-2.4	-4.7	-3.4	-5.2

As in the case presented in ref. [1] pressure drag forces are percentually larger than frictional ones. However, the frictional drag forces contribute more to the total drag for the present pod than for the pod in ref. [1]. The opposite trend, of course, occurs for the pressure-based contribution to the total resistance.

Applying the percentages of Table III to those in Table II the viscous and pressure components of the resistance can be obtained in absolute terms relative to the thrust of the model scale propulsion unit.

They are shown in Table IV. Both the pressure and frictional drag decrease for the pod and strut from model to full scale, the reduction in frictional drag being stronger.

7. Discussion

There are many parameters affecting the scaling of a podded propulsion unit, which make it difficult to predict the correct extrapolation factors to be applied in a particular case. Such factors depend not only on the shape and type of passive components in the unit, but also on the scale ratio, type of pod configuration (pusher/puller), location of propeller, propeller loading, etc. There is a clear tendency to rely more and more on CFD tools to assist model test experiments for this difficult task [5]. This is particularly necessary when the pod configuration is of a new type from which no information is available. A simple way of extrapolating model tests results is [4] to multiply the viscous resistance coefficient of the pod in model scale by a factor obtained from RANS computations. The scaling of small units as those presented in this paper requires larger factors than those traditionally used for appendage scaling.

For some pod configurations as that presented in this paper the distinction between the components is not evident and several definitions can be made. RANS extrapolation methods are not dependent on such definitions in their predictions of extrapolation factors as may be the case for some empirical methods.

8. Conclusions

RANS code FINFLO has been used to predict the performance at model and full scale of a Compact Azipod. Estimation of relative forces and propeller torque are shown for the different components of the pod unit as well as for the total unit. Pictures of pressure distributions and streamlines are presented. They illustrate regions of 3D separation on the strut and pod, and pressure distributions on both suction and pressure sides of the blades.

Over the last years RANS codes have been emerging as powerful scaling tools based on sound physics for the extrapolation of hydrodynamic resistance in podded propulsors. RANS code calculation results are needed before simple scaling formulae can be developed for the extrapolation of typical pod configurations.

9. Acknowledgements

The authors wish to thank *ABB Marine and Turbo-charging* for allowing this publication. Special thanks are given to Tomi Veikonheimo for providing the data subject to investigation.

10. References

1. Sánchez-Caja A, Ory E, Salminen E, Pylkkanen J, Siikonen T, (2003), "Simulation of Incompressible Viscous Flow Around a Tractor Thruster in Model and Full Scale", The 8th

International Conference on Numerical Hydrodynamics, Busan, Korea, September 22-25, 2003, 11 pp.

2. Sánchez-Caja A, Pylkkanen J, (2005), “Optimisation of Podded Propulsor for Fast Ropax Using RANS Solver with Cavitation Model”, International Conference on Fast Sea Transportation: FAST’2005, St.Petersburg, Russia, June, 2005, 11 pp.

3. Sánchez-Caja, A., Rautaheimo, P., Salminen, E., and Siikonen, T. (1999), "Computation of the Incompressible Viscous Flow around a Tractor Thruster Using a Sliding Mesh Technique", 7th International Conference in Numerical Ship Hydrodynamics, Nantes (France), 1999.

4. Lobatchev, M.P., Chicherin, I.A., (2001), “The Full-Scale Resistance Estimation for Podded Propulsion System by RANS Method.” Lavrentiev Lectures. Proceeding of International Symposium on Ship Propulsion. SP 2001. 19-21 June 2001, St.Petersburg, pp.39-44.

5. ITTC (2005), report of the Specialist Committee on Azimuthing Podded Propulsion, 24th International Towing Tank Conference, Edinburgh, Proceedings Vol.II, p 543-600.